



NISTIR 4674

An Analysis of Moisture Accumulation in a Wood Frame Wall Subjected to Winter Climate

D. M. Burch
W. C. Thomas



United States Department of Commerce
National Institute of Standards and Technology

QC
100
.U56
#4674
1991
C.2

NISTC
DC/DO
456
4674
1991
C.2

An Analysis of Moisture Accumulation in a Wood Frame Wall Subjected to Winter Climate

D. M. Burch
W. C. Thomas

October 1991



U.S. Department of Commerce
Robert A. Mosbacher, *Secretary*
National Institute of Standards and Technology
John W. Lyons, *Director*
Building and Fire Research Laboratory
Gaithersburg, MD 20899



Prepared for:
U.S. Department of Energy
Washington, D.C., 20858

TABLE OF CONTENTS

ABSTRACT	1
KEYWORDS	1
INTRODUCTION	1
THEORY	2
Governing Equations	3
Indoor Boundary Conditions	4
Outdoor Boundary Conditions	4
Interface between Two Storage Layers	5
Non-Storage Layer	5
Solution Procedure	6
MATERIAL PROPERTIES	6
Heat Transfer Properties	6
Diffusion Regime	7
Sorption Isotherms	7
Moisture Diffusivities	7
Capillary Regime	8
Liquid Diffusivity	8
Capillary Pressure	8
Unsaturated Liquid Permeability	9
Transition Regime	9
DISCUSSION OF RESULTS	10
Airtight Wall without a Vapor Retarder	10
Airtight Wall with a Vapor Retarder	11
Wall with a Vapor Retarder and Indoor Air Leakage	12
Effect of Other Construction Parameters	12
Orientation	12
Exterior Paint Permeance	12
Sheathing Permeance	13
Amount of Insulation	13
Using Outdoor Ventilation as a Moisture Management Technique	13
SUMMARY AND CONCLUSIONS	14
ACKNOWLEDGMENTS	15

NOMENCLATURE	15
REFERENCES	16

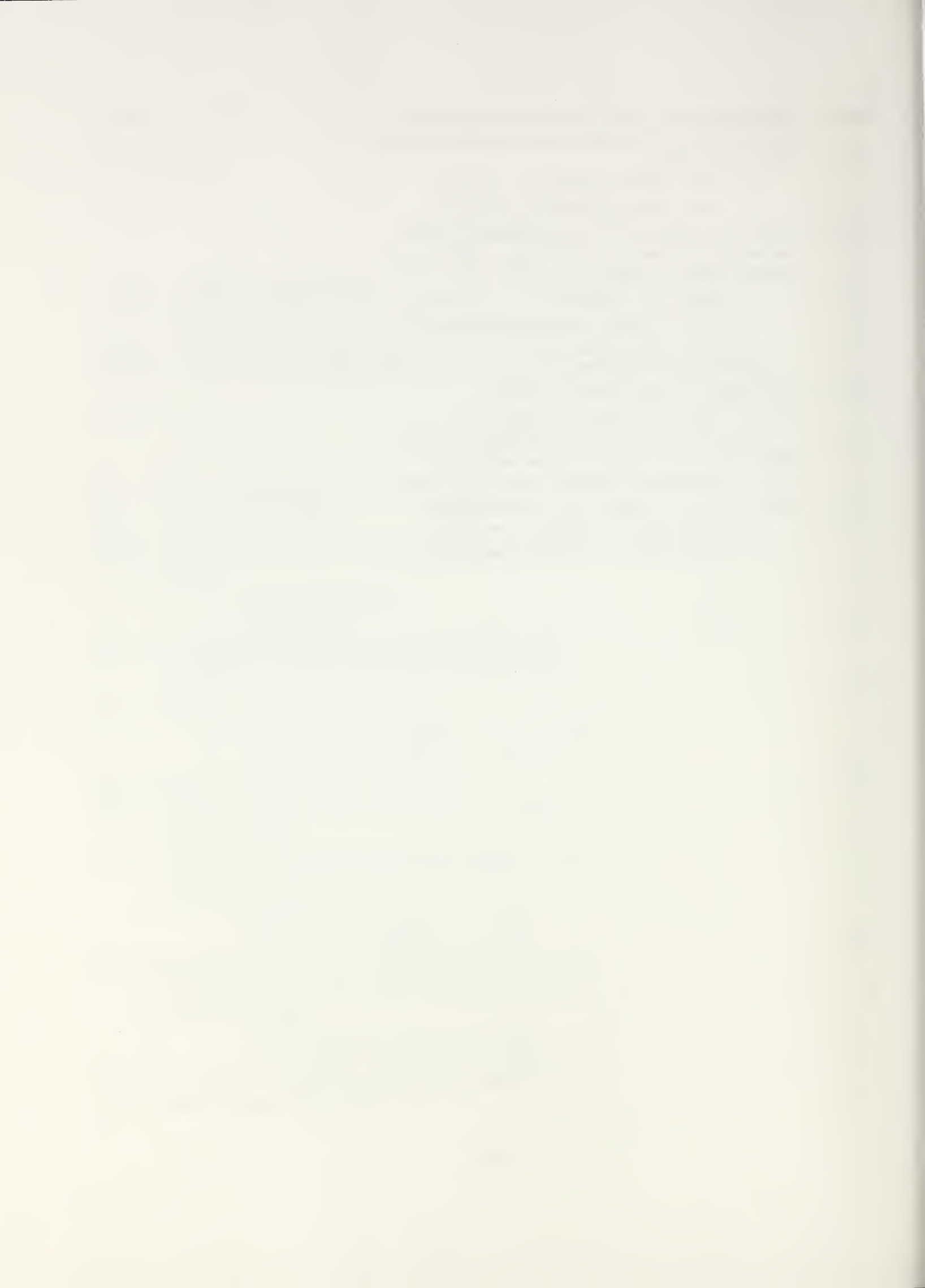
LIST OF TABLES

TABLE 1 Heat Transfer Properties	18
TABLE 2 Empirical Constants for Sorption Isotherm Function	18
TABLE 3 Empirical Constants for Permeability Function	18
TABLE 4 Permeances for Non-Storage Layers	19
TABLE 5 Dry Porosity and Saturated Liquid Permeability Values Used in Analysis . . .	19

LIST OF FIGURES

Fig. 1. Wall consisting of N layers	20
Fig. 2. The sorption isotherm	20
Fig. 3. A non-storage layer	21
Fig. 4. Diffusion properties of materials used in the analysis	
a. Sorption isotherms	
b. Permeabilities	22
Fig. 5. Dimensionless capillary pressure versus saturation of wetting fluid for unconsolidated sands [Collins (1961)]	23
Fig. 6. Moisture diffusivity for white pine	
a. Diffusivity for the moisture content gradient	
b. Diffusivity for the temperature gradient	24
Fig. 7. Wood frame wall used in the analysis	25
Fig. 8. Weekly average outdoor temperature for the three outdoor climates	25
Fig. 9. Moisture content plotted versus time of year for the wood frame wall without a vapor retarder and without indoor air leakage	
a. Indoor relative humidity, $\phi = 35\%$	
b. Indoor relative humidity, $\phi = 50\%$	26
Fig. 10. Moisture content plotted versus time of year for the wood frame wall with a vapor retarder and without indoor air leakage	
a. Indoor relative humidity, $\phi = 35\%$	
b. Indoor relative humidity, $\phi = 50\%$	27
Fig. 11. Illustration of indoor air leakage into insulation cavity of wood frame wall	28

Fig. 12.	Moisture content plotted versus time of year for the wood frame wall with a vapor retarder and with indoor air leakage	
	a. Indoor relative humidity, $\phi = 35\%$	
	b. Indoor relative humidity, $\phi = 50\%$	28
Fig. 13.	Moisture content plotted versus time of year for the wood frame wall without a vapor retarder and without indoor air leakage (Madison, WI)	
	a. Effect of orientation	
	b. Effect of exterior paint permeance	
	c. Effect of sheathing permeance	
	d. Effect of insulation	29
Fig. 14.	Illustration of wood frame wall with an exterior cavity ventilated with outdoor air	30
Fig. 15.	Comparison of moisture content variation of wood frame wall without outdoor ventilation (Fig. 7) versus that of the same wood frame wall with outdoor ventilation (Fig. 14) in Madison	
	a. Indoor relative humidity, $\phi = 35\%$	
	b. Indoor relative humidity, $\phi = 50\%$	30



ABSTRACT

A transient, one-dimensional, finite-difference model is presented that predicts the coupled transfer of heat and moisture in a multilayer wall under nonisothermal conditions. The model can predict moisture transfer in the diffusion through the capillary flow regimes. It has a provision to account for convective moisture transfer by including embedded cavities which may be coupled to indoor and outdoor air.

The model is subsequently used to predict the time-varying average moisture content in the sheathing and siding of a wood frame wall as a function of time of year. Results are shown for a mild winter climate (Atlanta, GA), an intermediate winter climate (Boston, MA), and a cold winter climate (Madison, WI). The indoor temperature is maintained at 21°C, and separate computer runs are carried out for indoor relative humidities of 35% and 50%.

The effect of several construction parameters on the winter moisture accumulation are investigated. The parameters include the interior vapor retarder permeance, sheathing permeance, exterior paint permeance, indoor air leakage, and the amount of insulation.

KEYWORDS: capillary transfer, moisture control guideline, moisture management in walls, moisture performance of walls, moisture transfer, water vapor diffusion

INTRODUCTION

During the winter season, the absolute humidity, or moisture content, of the air within a residence is considerably higher than that of the outdoor air. As a result, moisture permeates into walls by way of diffusion and air leakage through cracks in the interior surface. This moisture is partially adsorbed and accumulates within the outer material layers of the wall. In response to the seasonal variation in outdoor temperature, Dutt (1968) observed that the moisture content in outer wall layers builds up during cold winter periods and subsequently decreases during warm summer periods.

Seasonal moisture cycling of the outer wall layers causes wood-based materials to alternately expand and contract. Repeated moisture cycling often causes warped and bowed boards, delaminated plywood, pushed out nails, and the separation of wood members from the structure. Moreover, it may also weaken the bond between exterior paint and the substrate material, thereby giving rise to paint failure. In isolated cases, high moisture contents in building materials may cause fungus degradation. Moisture problems in walls have been documented in field surveys carried out by Tsongas (1990), Rose (1986), and Merrill and TenWolde (1989).

Relative to the above discussion, the maximum amount of sorbed (or bound) moisture that can be stored in a material when it is placed in an environment with a relative humidity approaching

100% is denoted "maximum sorption". Liquid water begins to appear in the pore structure of the material when its moisture content approaches and exceeds that of maximum sorption. The condition existing when all pore structures are completely filled with liquid water is called "saturation". For conifer softwoods typically used in building construction, the moisture content at maximum sorption is about 27% of the dry mass of wood and about 230% at saturation. Maximum sorption is generally regarded as the maximum amount of moisture that can be taken on by a material without degradation.

Experts often disagree on the cause and remedial action for moisture problems in residences. A contributing factor to this situation is that general analytical models have not been available to analyze moisture performance of building components. Mathematical models (e.g., Kohonen (1984), Andersson (1985), Kiessl (1983), Oosterhout and Spolek (1988), and Pedersen (1990)) for predicting time-dependent moisture transfer within building components are just currently evolving. Consequently, experimentation and related previous experience are often the only proven approaches available for addressing moisture problems while minimizing heat loss. Experimentation on individual components is, of course, costly and time-consuming. Moreover, specific results cannot be readily extended to different constructions and indoor/outdoor climatic conditions.

Burch and Thomas, et al. (1989) previously presented a distributed-moisture-capacity, finite-difference model that predicted the time-dependent moisture diffusion in a multilayer wall. This model was one-dimensional and used water vapor pressure as the potential for moisture transfer. The model was experimentally verified for a 3-layer wall tested under non-isothermal conditions. This previous model had the limitation that it did not include capillary or convective transfer. In the present paper, the earlier finite-difference model is extended to a more general formulation that includes these effects.

THEORY

A composite wall comprised of N layers in series that stores both heat and moisture is analyzed (see fig. 1). Initially, each layer has an arbitrary moisture content. The exterior surfaces of the wall are then exposed to ambient environments with time-varying temperatures and water vapor pressures. The variation in moisture content and temperature within each of the layers is sought as a function of time. The following assumptions are used in the analysis:

- The driving forces for moisture transfer are the gradients in the moisture content and temperature.
- Heat and moisture transfer is one-dimensional.
- The heat transfer properties are constant (i.e., not a function of temperature or moisture content).

- The sorption isotherm is based on the average of adsorption and desorption data. Hysteresis and temperature effects on the sorption isotherm are neglected.
- The effects of temperature and hysteresis on the relationship between suction pressure and moisture content are neglected.
- Vapor adsorption at a surface releases the latent heat of vaporization and vice versa.

Additional assumptions are introduced in the development which follows.

Governing Equations

Within each layer n of the wall shown in figure 1, moisture transfer is governed by the following conservation of mass equation¹:

$$\frac{\partial}{\partial y} \left[D_{\gamma}(\gamma, T) \frac{\partial \gamma}{\partial y} \right] + \frac{\partial}{\partial y} \left[D_T(\gamma, T) \frac{\partial T}{\partial y} \right] = \frac{\partial \gamma}{\partial t} \quad (1)$$

The selection of moisture content (γ) and temperature (T) as potentials has the advantage that the same mathematical formulation includes both diffusion transfer and capillary transfer, as will be shown later. This formulation is equivalent (as seen later) to using the gradient in vapor pressure as the moisture transfer potential in the diffusion regime and suction pressure in the capillary flow regime, with a single required diffusivity.

Heat transfer is governed by the conservation of energy equation:

$$\frac{\partial}{\partial y} \left[k(\gamma, T) \frac{\partial T}{\partial y} \right] = \rho(C_d + \gamma C_w) \frac{\partial T}{\partial t} \quad (2)$$

Enthalpy transport by moisture movement in a wall system is generally small and therefore is neglected in the present analysis. However, latent transport of heat is included in the boundary conditions as will be discussed later. The term $(C_d + \gamma C_w)$ includes the effect of energy storage in both the dry material and accumulated moisture. The effect of accumulated moisture can be important (e.g., the specific heat of wood is increased by 69% after it adsorbs moisture from air at a relative humidity of 100%).

In the above two governing equations, strong couplings exist between heat and moisture transfer. Both the diffusivity for the moisture gradient (D_{γ}) and the diffusivity for the temperature gradient (D_T) are strong functions of moisture content and temperature. The thermal conductivity (k) can be a function of moisture content and temperature, but for the present analysis it is assumed to be constant.

¹ Symbols are defined in the Nomenclature.

Indoor Boundary Conditions

At the left boundary of the multilayer wall of figure 1, the convective heat transfer from the indoor air plus the latent heat from adsorbed or desorbed water vapor is equated to heat conduction into the surface, giving:

$$h_i(T_i - T) + \dot{n}_i \lambda = -k \frac{\partial T}{\partial y} \quad \text{at } y = 0 \quad (3)$$

At the same boundary, the moisture transferred through an air film and paint layer is equated to moisture transferred into the surface, or:

$$M_{ei}(P_i - P) = -\rho_d D_\gamma \frac{\partial \gamma}{\partial y} - \rho_d D_T \frac{\partial T}{\partial y} \quad \text{at } y = 0 \quad (4)$$

Here, an effective conductance (M_{ei}) defined by:

$$\frac{1}{M_{ei}} = \frac{1}{M_{fi}} + \frac{1}{M_{pi}} \quad (5)$$

has been introduced. The effect of a thin vapor retarder, such as paint or a vinyl covering, is taken into account as a surface conductance (M_{pi}) in series with the convective mass transfer coefficient (M_{fi}) associated with the air film.

In equation (4), the sorption isotherm function (f), defined below, is used as a constitutive relation to evaluate the boundary condition.

$$\gamma = f(\phi, T) \approx f(\phi) = f\left(\frac{P_v}{P_g}\right) \quad (6)$$

A sorption isotherm is illustrated in figure 2. The moisture content of a porous material at a relative humidity of 97% may be measured and is therefore known. Moreover, when a porous material is fully saturated with liquid water, the relative humidity within the pore structure is 100%. When less than fully saturated with water, the relative humidity is less than 100% due to the presence of curved menisci within the pore structure. For the present analysis, a straight line is used to connect the moisture contents just above maximum sorption ($\phi = 97\%$) and the state of saturation ($\phi = 100\%$).

Outdoor Boundary Conditions

Similarly, at the right boundary shown in figure 1, the boundary conditions for heat and moisture transfer are:

$$h(T - T_o') + \dot{n}_o \lambda = -k \frac{\partial T}{\partial y} \quad \text{at } y = L \quad (7)$$

and

$$M_{eo}(P - P_o) = -\rho_d D_\gamma \frac{\partial \gamma}{\partial y} - \rho_d D_T \frac{\partial T}{\partial y} \quad \text{at } y = L \quad (8)$$

These boundary conditions are evaluated in a similar fashion as those at the indoor surface given in equations (3) and (4).

Interface between Two Storage Layers

When the heat transfer at the interface between two storage layers is evaluated, the temperature is assumed to be continuous. When the moisture transfer is evaluated, the relative humidity is assumed to be continuous, and the sorption isotherm function (f), illustrated in figure 2, provides the constitutive relationship, or:

$$\phi = f_n^{-1}(\gamma_n) = f_{n+1}^{-1}(\gamma_{n+1}) \quad (9)$$

where the subscripts n and $n+1$ refer to the adjoining regions. The relative humidity is continuous at an interface, but the moisture content will generally be discontinuous.

Non-Storage Layer

The mathematical model has the provision for including non-storage layers (e.g., an air space, a glass-fiber insulation cavity, or a vapor retarder) that are sandwiched between two storage layers. In a non-storage layer, the storage of heat and moisture is neglected, and the transfers are steady. A non-storage layer may be convectively coupled to indoor and outdoor air.

Consider the non-storage layer shown in figure 3. At the interface between the non-storage layer and the adjacent storage layer to the right, the heat transferred through the non-storage layer plus the heat gains by convective exchange with the indoor and outdoor air and the latent heat from adsorbed or desorbed water vapor are equated to the heat conduction into the storage layer, or:

$$\begin{aligned} \frac{T_{s,n-1} - T_{s,n}}{R} + \dot{V}_i C \rho_a (T_i - T_{s,n}) + \dot{V}_o C \rho_a (T_o - T_{s,n}) + \dot{n}_s \lambda \\ = -k \frac{\partial T}{\partial y} \quad \text{at } y = y_s \end{aligned} \quad (10)$$

For the moisture, the diffusion transfer through the non-storage layer plus the moisture gains due to convective exchange with the indoor and outdoor air are equated to the moisture transfer into the storage layer, or:

$$\begin{aligned}
M(P_{s,n-1} - P_{s,n}) + \frac{0.622 \dot{V}_i \rho_a}{P_a} (P_i - P_{s,n}) + \frac{0.622 \dot{V}_o \rho_a}{P_a} (P_o - P_{s,n}) \\
= -\rho_d D_\gamma \frac{\partial \gamma}{\partial y} - \rho_d D_T \frac{\partial T}{\partial y} \quad \text{at } y = y_s
\end{aligned} \tag{11}$$

The sorption isotherm function (f) given in equation (6) is used as a constitutive relation in evaluating the above equation.

Solution Procedure

Equations (1-11) were recast into finite-difference equations using a uniform nodal spacing within each layer. An implicit solution technique with coupling between the two conservation equations was used to solve the equations. A FORTRAN 77 computer program, called MOIST, with a tridiagonal-matrix solution algorithm was prepared. At each time step, the calculation proceeds by first solving for the temperature distribution. Next, a set of surface moisture contents are calculated, followed by a set of the interior moisture contents. Next, a revised set of surface moisture contents and interior moisture contents are calculated based on the new values of the diffusion coefficients, and so forth. This process is repeated until convergence of the moisture contents is attained. By choosing a sufficiently small time step, the need to iterate between the temperature and moisture solutions was eliminated.

The accuracy of the numerical solution depends on both the nodal spacing and the time step. Progressively smaller nodal spacing and time steps were used to ensure that calculated results did not depend significantly on the space or time increment.

Later in the paper, program MOIST is used to analyze the moisture transfer in a wood frame wall. For this analysis, a time step of one hour is used. The number of nodes was 3 in the gypsum board, 5 in the sheathing, and 5 in the wood siding. The insulation was treated as a non-storage layer. When the computer program was run on a Model 386 personal computer, equipped with a math co-processor and having a 33 Mhz clock speed, 30 minutes of calculation time was required to simulate one year of real time.

MATERIAL PROPERTIES

Heat Transfer Properties

The thermal conductivity, density, and specific heat for the various building materials used in the analysis were taken from ASHRAE (1989) and are summarized in table 1. The glass-fiber insulation was treated as a non-storage layer and was assumed to have a thermal resistance of

1.9 m²·°C/W. The thermal resistances of kraft paper and the paint layers were neglected because these layers are very thin.

Diffusion Regime

In the regime below maximum sorption, free liquid water is not present in the pore structure. Here the term free liquid water denotes water that may be removed by body forces when a material is spun in a centrifuge. It does not include capillary condensation which is bound in the micropores of the material. Procedures used to obtain sorption isotherms and vapor diffusivities for the materials are discussed below.

Sorption Isotherms. The sorption isotherm data used in the analysis were taken from Richards, et al. (1992) where sorption isotherm data were fit to an equation of the form:

$$\gamma = \frac{a_1\phi}{(1 + a_2\phi)(1 - a_3\phi)} \quad (12)$$

where a_1 , a_2 , and a_3 are empirical constants determined by a regression analysis of the measured data. The empirical coefficients are summarized in table 2, and sorption isotherm curves for the materials are given in figure 4a.

Moisture Diffusivities. The water-vapor diffusivities for the materials are based on permeability measurements carried out by Burch, et al. (1992). For each material, a series of permeability cup measurements were carried out. In the measurements, small relative humidity differences were imposed across the specimens, and a functional relationship was established between permeability and the average relative humidity across the specimen. Separate measurements carried out at 24° and 7°C revealed that temperature had an insignificant effect on permeability. In this study, the permeability data were fit to an equation of the form:

$$\mu = \exp(a_1 + a_2\phi + a_3\phi^2) \quad (13)$$

where a_1 , a_2 , and a_3 are empirical constants determined from a fit of the measured data. The empirical coefficients are summarized in table 3. A plot of the permeabilities for the materials used in the analysis are given in figure 4b.

The diffusivity for the moisture gradient (D_γ) and the diffusivity for the temperature gradient (D_T) were calculated by the relations:

$$D_{\gamma} = \frac{\mu(\phi)P_{vg}(T)}{\rho_d \frac{\partial f(\phi)}{\partial \phi}} \quad \text{and} \quad D_T = \frac{\mu(\phi)\phi \frac{\partial P_{vg}(T)}{\partial T}}{\rho_d} \quad (14)$$

The above equations may be derived by introducing the sorption isotherm function and applying the chain rule to Fick's steady-state diffusion equation with the gradient of the water-vapor pressure as the driving-force potential.

The glass-fiber insulation, the 19-mm-wide air space, the paint layers, and the kraft paper vapor retarder were treated as non-storage layers. Permeances for these materials are based on ASHRAE (1989) and are given in table 4.

Capillary Regime

Capillary transfer occurs when a contiguous path of liquid exists within the porous material. As the moisture content of a material is increased above maximum sorption, the moisture content at which a contiguous path of liquid first exists is termed "irreducible saturation."

Liquid Diffusivity. In the capillary flow regime, the liquid diffusivity in porous materials may be predicted by:

$$D_{\gamma} = -\frac{\rho_w \kappa \frac{\partial P_c}{\partial \gamma}}{\rho_d \nu} \quad (15)$$

This equation follows by applying the chain rule to Darcy's Law for liquid flow through a porous media. In the analysis, the density of water (ρ_w) was taken to be 1000 Kg/m³, and the viscosity of water (ν) was taken to be 7.25 X 10⁻⁴ Pa·s. Procedures to obtain the capillary pressure (P_c) and the unsaturated liquid permeability (κ) are discussed below.

Capillary Pressure. The Leverett "j-function" (Leverett 1941) is accepted by various authors in different fields as a generalized dimensionless functional form that may be used to correlate the capillary pressure with moisture content for many different materials. The Leverett j-function is defined by:

$$j = \frac{P_c}{\sigma} \sqrt{\frac{\kappa_s}{\epsilon_d}} \quad (16)$$

where κ_s is the liquid permeability of the porous material at a saturated moisture content and σ is the surface tension of water, taken as 69.2 X 10⁻³ N/m. Dry porosity (ϵ_d) and saturated liquid permeability values (κ_s) used in the analysis are given in table 5.

The Leverett j-function or the dimensionless capillary pressure is plotted as a function of the saturation of the wetting fluid in figure 5. Here the saturation of the wetting fluid (S) is defined as:

$$S = \frac{\gamma - \gamma_{ir}}{\gamma_s - \gamma_{ir}} \quad (17)$$

The Leverett j-function was curve fitted to data as shown in figure 5.

Unsaturated Liquid Permeability. The unsaturated liquid permeability (κ) was estimated by the linear relation:

$$\kappa = \kappa_s S \quad (18)$$

The above equation is based on the modeling work of Stanish, et al. (1985). Note that the unsaturated liquid permeability is equal to zero at irreducible saturation and equal to the saturated liquid permeability (κ_s) at a fully saturated state.

The liquid diffusivity was calculated from equation (15) using the above procedures to estimate the derivative of the capillary pressure and the unsaturated permeability. The authors recognize that this procedure provides only engineering estimates for the liquid diffusivity of materials. However, liquid diffusivity data for building materials is seriously lacking in the literature. NIST is currently measuring liquid diffusivities for building materials. As these measurement results become available, they will be incorporated into the model and replace the approximate method outlined above.

Within the capillary flow regime, the diffusivity for the temperature gradient (D_T) was calculated using equation (14).

Transition Regime

When the moisture content of a material is between a state of maximum sorption and irreducible saturation, the material is said to be in a "transition regime." At and below the irreducible saturation moisture content, free liquid water exists but not in a contiguous path. In this regime, the capillary attraction between discrete liquid particles and pores is so strong that this liquid cannot be separated from the porous material by ordinary mechanical means, such as centrifuging or applying a pressure gradient across the material. In this regime, capillary transfer vanishes and the water vapor pressure approaches saturation.

To date, different researchers do not agree on the exact moisture transfer mechanism, especially in an isothermal situation. The present model uses moisture concentration and temperature gradients as the moisture transfer potential in this regime. The diffusivity for the moisture

gradient (D_γ) was estimated as a function of moisture content by joining the diffusivity curves in the diffusion and capillary regimes with a straight line (on a logarithmic scale) as shown in figure 6a. The mathematical relationship for the diffusivity in the transition regime is then:

$$D_\gamma = D_{ms-} \text{Exp} \left[\frac{\gamma - \gamma_{ms-}}{\gamma_{ir+} - \gamma_{ms-}} \ln \left(\frac{D_{ir+}}{D_{ms-}} \right) \right] \quad (19)$$

In the above equation, D_{ms-} is the left hand limit of diffusivity at maximum sorption and D_{ir+} is the right hand limit of liquid diffusivity at irreducible saturation. Note that equations (14), (15), and (19) provide a continuous model for the moisture diffusivity from a dry to a saturated state.

The diffusivity for the temperature gradient (D_T) was also calculated by equation (14) and is shown in figure 6b.

DISCUSSION OF RESULTS

The above mathematical model was used to predict the seasonal variation in the moisture content of the sheathing and wood siding of the wood frame wall shown in figure 7. This wall was comprised of 13-mm-thick gypsum board covered with latex paint, a 92-mm-thick glass-fiber insulation, 13-mm-thick fiber-board sheathing, and 13-mm-thick wood siding covered with oil-base paint.

In the analysis, the indoor temperature was maintained at 21°C. The outdoor temperature, relative humidity, and solar radiation were taken from WYEC hourly weather data [Crow 1981] for a mild winter climate (Atlanta, GA), an intermediate winter climate (Boston, MA), and a cold winter climate (Madison, WI). The heating degree days for these cities are 1,706°C·days for Atlanta, 3207°C·days for Boston, and 4228°C·days for Madison. Weekly average outdoor temperatures for these three cities are given in figure 8. Six months of weather data were used to initialize the simulation results so that they would be independent of assumed initial moisture content and temperature.

Airtight Wall without a Vapor Retarder

Winter moisture accumulation in an airtight (i.e., no convection) wood frame wall without a vapor retarder is plotted versus time of year in figure 9a for an indoor relative humidity of 35% and in figure 9b for an indoor relative humidity of 50%. In each plot, the solid line depicts the average moisture content of the wood siding, while the broken line depicts the average moisture content in the fiber-board sheathing. In the figures, maximum sorption for the wood siding is depicted by the solid horizontal lines and that for the sheathing by the dashed horizontal line. As indicated earlier, when the moisture content is above maximum sorption, free liquid water

exists within the pores of a material, and serious problems are expected if this condition exists over an extended period of time.

Comparing the pairs of curves for the three different climates in figure 9a, higher moisture contents are seen to occur in colder climates. In actual houses, the effect of climate will be less pronounced because the indoor relative humidity in houses tends to decrease in colder climates as a result of increased moisture losses from window condensation and infiltration of drier air. It is also interesting to note that the peak moisture content occurs about two months after the minimum outdoor temperature shown in Fig 8.

Comparing Figs. 9a and 9b, indoor relative humidity is seen to be a highly significant parameter affecting winter moisture accumulation. Increasing the indoor relative humidity from 35% to 50% substantially increases the moisture accumulation. When the indoor relative humidity was 35% (see fig. 9a), the moisture contents of the sheathing and wood siding were always below maximum sorption. On the other hand, when the indoor relative humidity was increased to 50% (see fig. 9b), the moisture contents approached maximum sorption in Boston and rose considerably above maximum sorption for 4-6 months in Madison.

These large seasonal variations in moisture content will cause wood-based products to undergo expansion and contraction cycles which contribute to material degradation.

The results in figure 9 and with the same type of results following show that peak moisture accumulation in various materials generally do not exceed maximum sorption by much and, in fact, never reach the capillary flow regime. This situation means that the overall results are relatively insensitive to the significant uncertainties in material properties above maximum sorption.

Airtight Wall with a Vapor Retarder

A vapor retarder, placed between the gypsum board and the insulation, was added to the wall used in the two previous computer simulations. The vapor retarder consisted of a kraft paper having a permeance of $1.7 \times 10^{-11} \text{ kg/s} \cdot \text{m}^2 \cdot \text{Pa}$. The simulation results with this vapor retarder are given in figure 10 for the same two indoor relative humidity conditions.

Comparing Figs. 9 and 10, the vapor retarder is seen to provide a significant reduction in the seasonal cycles in moisture content. Note that the moisture content in both the sheathing and wood siding is always maintained below 12% even for the higher indoor relative humidity. This reduces the seasonal expansion and contraction cycles in wood-based products, thereby reducing material degradation due to moisture cycling. These results indicate that a vapor retarder is an effective means of controlling moisture accumulation in a wood frame wall exposed to cold climates.

Wall with a Vapor Retarder and Indoor Air Leakage

The mathematical model was next used to investigate the effect of indoor air leakage on the moisture accumulation within the wood frame wall with a vapor retarder (see fig. 11). In the analysis, the insulation cavity was ventilated with indoor air at an assumed rate of one volume change/h. Convective air exchange occurs due to air leakage paths associated with electrical outlet boxes, baseboard cracks, and other inherent penetrations.

The moisture contents of the wood siding and fiber-board sheathing are plotted versus time of year in figure 12a for an indoor relative humidity of 35% and in figure 12b for an indoor relative humidity of 50%. For an indoor relative humidity of 50%, the moisture contents are seen to approach maximum sorption in Madison. It should be pointed out that this analysis is one-dimensional and does not include the effect of higher sheathing moisture contents directly in line with impinging air leakage. The effect of convective transport is averaged over the entire sheathing surface.

The results of figure 12 suggest that indoor air leakage is also an important moisture transfer mechanism. Comparing the results of Figs. 10 and 12, indoor air leakage is seen to substantially increase the moisture content in a wall with a typical vapor retarder. These results indicate that in order to reduce moisture accumulation in a wood frame wall exposed to cold climate, it is also necessary to seal interior air leakage paths.

It should be pointed out that the above analysis is very dependent on an assumed cavity ventilation rate of one volume change/h. This value was not based on measured data, but rather an engineering estimate that seemed reasonable to the authors.

Effect of Other Construction Parameters

In this section, a sensitivity analysis, using the wood frame wall of figure 7, is carried out to investigate the effect of orientation, exterior paint permeance, exterior sheathing permeance, and the amount of insulation. In the analysis, the wall is exposed to an indoor relative humidity of 35% and the outdoor weather of Madison, WI.

Orientation. The moisture contents of the sheathing and siding of a north-facing and south-facing wall are compared in figure 13a. The higher solar radiation for the south-facing wall causes its moisture contents to be lower than those for an identical north-facing wall. The peak wood moisture content in the south-facing wall is 0.04 lower than for the identical north-facing wall.

Exterior Paint Permeance. In figure 13b. the moisture accumulation within the wood frame wall with exterior oil-base paint is compared to the same wall with a considerably more permeable latex paint. The permeance of the latex paint was $5.7 \times 10^{-10} \text{ kg/s} \cdot \text{m}^2 \cdot \text{Pa}$, and that for the oil-base paint was $1.1 \times 10^{-10} \text{ kg/s} \cdot \text{m}^2 \cdot \text{Pa}$.

The results indicate that the use of exterior latex paint, as opposed to oil-base paint, enhances the escape of moisture during warm drying periods, and thereby maintains somewhat lower moisture contents in the wood siding. The peak wood moisture content in the wall painted with latex paint is seen to be 0.03 lower than the same wall painted with oil-base paint.

Sheathing Permeance. The moisture accumulation for a wood frame wall with fiber-board sheathing is compared to that for the same wall with the considerably less permeable plywood sheathing. The permeance of the fiber-board sheathing was about 150 times that of the plywood. The results are given in figure 13c.

The results indicate that the use of less permeable plywood sheathing reduced the ingress of moisture into the wood siding. The peak moisture content in the wood siding for the wall with plywood sheathing was 0.05 lower than that for the same wall with fiber-board sheathing. Note that the moisture content of the two sheathing materials do not differ much.

Amount of Insulation. In figure 13d, the moisture accumulation in a wood frame wall without insulation is compared to the same wall with insulation. When the thermal insulation is in the wood frame wall, most of the inside-to-outside temperature difference occurs across the insulation, and a small temperature difference occurs between the sheathing and wood siding. This causes the moisture content of the sheathing and siding not to be much different. On the other hand, when the thermal insulation is absent from the wall, a much larger temperature difference occurs between the sheathing and wood siding. This causes moisture to move from the warmer sheathing outwards into the colder wood siding. This result indicates that when uninsulated wood frame walls are retrofitted with thermal insulation in cold climates, the sheathing materials will tend to have increased moisture content.

Using Outdoor Ventilation as a Moisture Management Technique

Another moisture management technique for wood frame walls is the use of outdoor ventilation to remove accumulated moisture instead of using an interior vapor retarder and sealing interior air leakage paths. Here a 19-mm naturally-ventilated cavity is formed between the sheathing and wood siding as shown in figure 14. In the analysis, the cavity ventilation rate was assumed to be 6 volume changes/h.

The results of the analysis are given in figure 15a for an indoor relative humidity of 35% and in figure 15b for an indoor relative humidity of 50%. In each figure, the following three cases are compared: the original wood frame wall shown in figure 7, the wood frame wall with an unventilated air cavity, and the wood frame wall with the ventilated air cavity shown in figure 14.

These results show that, when the sheathing and siding are in contact, the moisture content of the sheathing and wood siding are not much different. When an unventilated air space is placed between the sheathing and wood siding, the moisture content of the wood siding increases and the moisture content of the sheathing decreases. This effect is caused primarily by the thermal

resistance of the air space altering the temperature distribution within the construction (i.e., the wood siding becomes colder and the sheathing becomes warmer). The larger temperature difference between the wood siding and sheathing causes accumulated moisture to redistribute towards the colder wood siding. When the air space is ventilated, the moisture content of both the sheathing and the wood siding decrease.

Comparing Figs. 15 and 10, it is seen that the use of outdoor ventilation is considerably less effective in reducing seasonal fluctuations in moisture content compared to the practice of providing a vapor retarder and sealing air leakage paths at the interior surface.

SUMMARY AND CONCLUSIONS

A mathematical model that predicts the combined transfer of heat and moisture in walls was presented. The model is one-dimensional and includes diffusion, capillary, and convective transfer. The model was used to analyze the winter moisture accumulation in a wood frame wall exposed to a mild winter climate (Atlanta, GA), an intermediate winter climate (Boston, MA), and a cold winter climate (Madison, WI).

Seasonal changes in outdoor temperature were found to produce seasonal variations in the moisture content of the outer layers of a wood frame wall. The most important parameters affecting the amount of moisture accumulation during the winter were the indoor relative humidity and the outdoor climate. Indoor relative humidity was observed to be more important than outdoor climate. The amount of moisture accumulation was larger in colder climates. Other parameters found to have a less important effect on the moisture accumulation were wall orientation, exterior paint permeance, and sheathing permeance. The addition of insulation to an uninsulated wood frame wall was found to significantly increase the moisture content of fiber-board sheathing.

Both diffusion and indoor air leakage were shown to be important mechanisms for transporting moisture. In walls without an interior vapor retarder, moisture diffusion was shown to accumulate sufficient moisture to produce free liquid water in the sheathing and wood siding of an airtight wall exposed to an indoor relative humidity of 50% and outdoor climate of Madison, WI. The leakage of indoor air into the insulation cavity of a wood frame wall with an interior vapor retarder was observed to accumulate moisture that approached a state of free liquid water.

The inclusion of a vapor retarder and sealing air leakage paths at the interior wall surface were found to decrease significantly seasonal variations in moisture contents, thereby preventing large expansion and contraction cycles in wood-based products that are believed to degrade the construction. The practice of using outdoor ventilation in a cavity between the sheathing and siding was found to be less effective than the practice of including a vapor retarder and sealing interior air leakage paths.

ACKNOWLEDGMENTS

The authors thank the Office of Buildings and Community Systems of the Department of Energy for funding this research study. The authors would like to acknowledge the helpful discussions with O.A. Plumb on capillary transfer.

NOMENCLATURE

Symbol	Units	Definition
a_n		Constants in sorption isotherm and permeability function ($n=1,2$, and 3)
C	$\text{J/kg} \cdot ^\circ\text{C}$	Specific heat
D_γ	m^2/s	Diffusivity for moisture gradient
D_T	$\text{kg}_w \cdot \text{m}^2/\text{kg}_d \cdot ^\circ\text{C} \cdot \text{s}$	Diffusivity for temperature gradient
f	kg_w/kg_d	Sorption isotherm function
h	$\text{W}/\text{m}^2 \cdot ^\circ\text{C}$	Surface heat transfer coefficient
j		Dimensionless capillary pressure
k	$\text{W}/\text{m} \cdot ^\circ\text{C}$	Thermal conductivity of porous material
L	m	Thickness of wall
M	$\text{kg}_w/\text{s} \cdot \text{m}^2 \cdot \text{Pa}$	Permeance or moisture conductance
\dot{m}''	$\text{kg}/\text{m}^2 \cdot \text{s}$	Moisture mass flux
P	Pa	Pressure
R	$\text{m}^2 \cdot ^\circ\text{C}/\text{W}$	Thermal resistance
S		Saturation of wetting fluid (see equation 17)
t	s	Time
T	$^\circ\text{C}$	Temperature
T_o'	$^\circ\text{C}$	Sol-air temperature
y	m	Distance from inside surface of wall
\dot{V}	m^3/s per m^2	Volumetric air flow rate per unit area
γ	kg_w/kg_d	Moisture content on dry basis
ϵ		Porosity
κ	m^2	Unsaturated liquid permeability
λ	J/kg_w	Latent heat of vaporization
μ	$\text{kg}_w/\text{s} \cdot \text{m}^2 \cdot \text{Pa}$	Water-vapor permeability
ν	$\text{Pa} \cdot \text{s}$	Viscosity of water
ρ	kg/m^3	Density
σ	N/m	Surface tension of water
ϕ		Relative humidity

Subscripts Refer to:

a	=	Atmospheric or air property
c	=	Capillary
d	=	Dry property
e	=	Effective property
f	=	Air film
g	=	Saturated state
i	=	Indoor or inside surface property
ir	=	Irreducible saturation
ms	=	Maximum sorption
n	=	Storage layer index
o	=	Outdoor property
p	=	Paint property
s	=	Surface value or liquid saturated state
T	=	Temperature gradient
v	=	Vapor property
w	=	Moist or water property
γ	=	Moisture content gradient

REFERENCES

Andersson, A.C. 1985. "Verification of calculation methods for moisture transport in porous building materials." Document D6:1985 (ISBN 91-540-4325-5). Swedish Council for Building Research, Stockholm, Sweden.

ASHRAE 1989. ASHRAE handbook - 1989 fundamentals, ch. 22. Atlanta: American Society of Heating, Refrigerating, and Air-Conditioning Engineers, Inc.

Burch, D.M., Thomas, W.C., Mathena, L.R., Licitra, B.A., and Ward, D.B. 1989. "Transient moisture and heat transfer in multilayer non-isothermal walls - comparison of predicted and measured results." Proceedings on the Conference on the Thermal Performance of the Exterior Envelopes of Buildings IV, Orlando, FL, Dec. 4-7, pp.513-531.

Burch, D.M., Thomas, W.C., and Fanney, A.H. 1992. "Water-vapor permeability measurements of common building materials," ASHRAE Transactions in review.

Collins, R.E. 1961. Flow of Fluids through Porous Materials. NY: Reinhold, pp. 31-33.

Crow, L.W. 1981. "Development of Hourly Data for Weather Year for Energy Calculations (WYEC)." ASHRAE Journal, Vol. 23, No. 10, October, pp. 37-41.

Dutt, J.E. 1968. "Moisture distribution in wood-frame walls in winter." Forest Products Journal, Vol. 18, No. 1, January.

Kiessl, K. 1983. "Kapillarer and dampfformiger feuchtetransport in mehrschichtigen bauteilen." Dissertation zur Erlangung des Grades Doktor-Ingenieur des Fachbereiches Bauwesen der Universitat-Gesamthochschule-Essen.

Kohonen, R. 1984. "A method to analyze the transient hygrothermal behavior of building materials and components," Publication 21. Technical Research Centre of Finland, Laboratory of Heating and Ventilation. October.

Leverett, M.C. 1941. "Capillary behavior in porous solids." AIME Transactions, Vol. 142, pp. 152-169.

Merrill, J.L. and TenWolde, A. 1989. "Overview of moisture-related damage in one group of Wisconsin manufactured homes.", ASHRAE Transactions, V. 95, Part 1.

Oosterhout, G.O. and Spolek, G.A. 1988. "Transient heat and mass transfer in layered walls." Proceedings of ASME Symposium on Heat and Mass Transfer in Insulation Systems.

Pedersen, C.R. 1990. "Combined heat and moisture transfer in building constructions," Report No. 214. Technical University of Denmark, Thermal Insulation Laboratory. Lyngby.

Richards, R.F.; Burch, D.M.; and Thomas, W.C. 1992. "Water vapor sorption measurements of common building materials." ASHRAE Transactions, in review.

Rose, W.B. 1986. "Moisture damage to homes in Champaign, IL." Proceedings of the Symposium on Air Infiltration, Ventilation, and Moisture Transfer, Ft. Worth, TX, Dec. 2-4, pp. 198-211.

Stanish, M.A., Schajer, G.S., and Kayihan, F 1985. Mathematical Modeling of Wood Drying from Heat and Mass Transfer Fundamentals. Drying '85, Hemisphere Publications, New York.

Tsongas, G. 1990. "The Northwest wall moisture study: a field study of excess moisture in walls and moisture problems and damage in new northwest homes," Report No. DOE/BP-91489-1. Bonneville Power Administration. June.

TABLE 1 Heat Transfer Properties			
Material	Thermal Conductivity	Density kg/m ³	Specific Heat J/kg · °C
Plywood	0.118	545	1214
Wood Siding	0.118	365	1633
Gypsum Board	0.160	670	1098
Fiber-Board Sh.	0.0663	352	1298

TABLE 2 Empirical Constants for Sorption Isotherm Function			
Material	a ₁	a ₂	a ₃
Plywood	0.3441	6.177	0.8283
Wood Siding	0.1936	2.095	0.7687
Gypsum Board	0.02465	9.0750	0.93540
Fiber-Board Sh.	2.7136	65.267	0.8684

TABLE 3 Empirical Constants for Permeability Function			
Material	a ₁	a ₂	a ₃
Plywood	-30.10	3.2963	2.4391
Wood Siding	-28.68	-0.9198	4.5776
Gypsum Board	-23.470	-1.4799	1.0816
Fiber-Board Sh.	-24.09	0.1836	-0.3919

TABLE 4 Permeances for Non-Storage Layers	
Material	$10^{-10} \text{ kg}_w/\text{s} \cdot \text{m}^2 \cdot \text{Pa}$
Latex Paint	5.7
Oil-Base Paint	1.1
92 mm Glass Fiber Ins.	18.
Kraft Paper (Asphalt Impreg.)	0.17
19 mm Air Space	69.

TABLE 5 Dry Porosity and Saturated Liquid Permeability Values Used in Analysis		
Material	ϵ_d	$\frac{\kappa_s}{\text{m}^2}$
Plywood	0.636	1.4×10^{-20}
Wood Siding	0.756	2.8×10^{-19}
Fiber-Board Sh.	0.765	3.9×10^{-15}

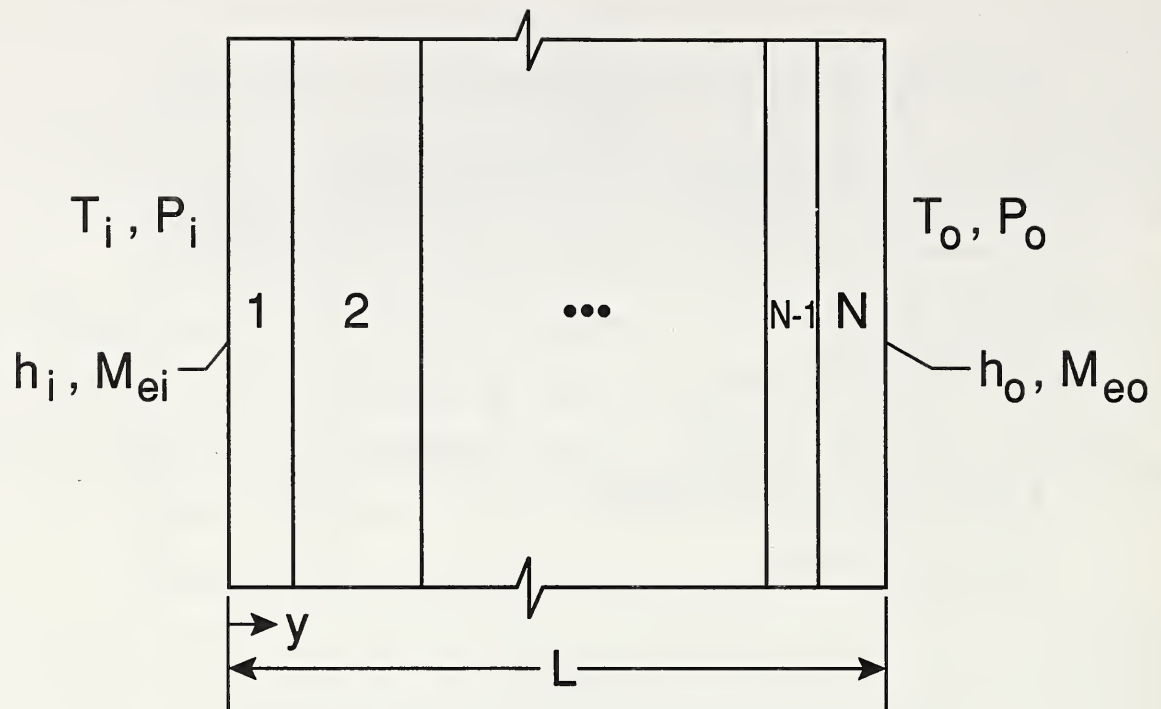


Fig. 1. Wall consisting of N layers

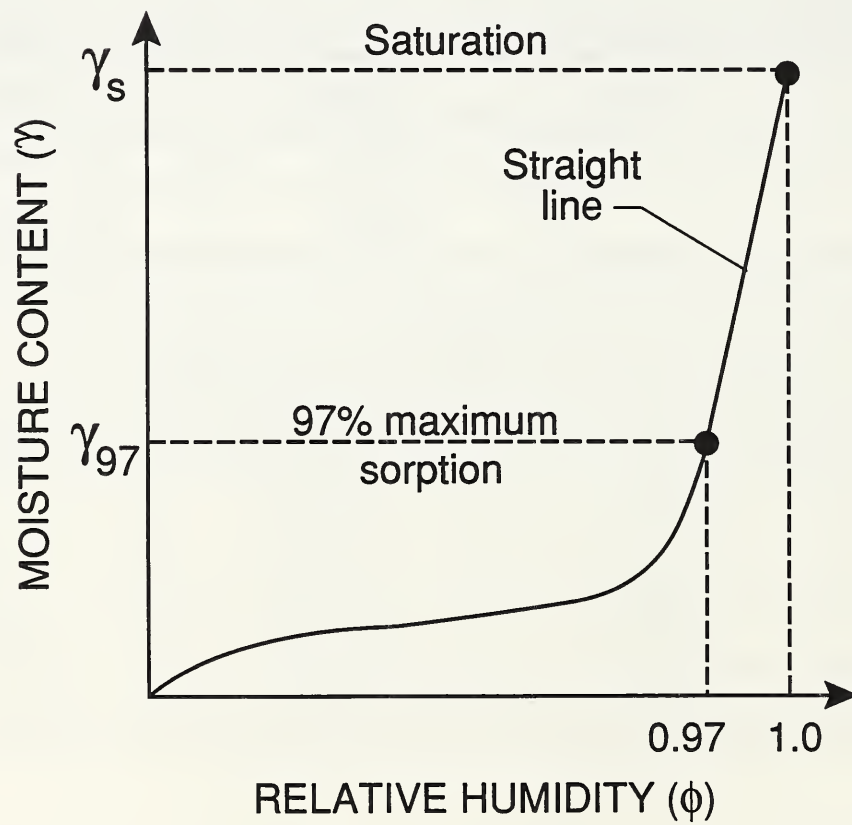


Fig. 2. The sorption isotherm

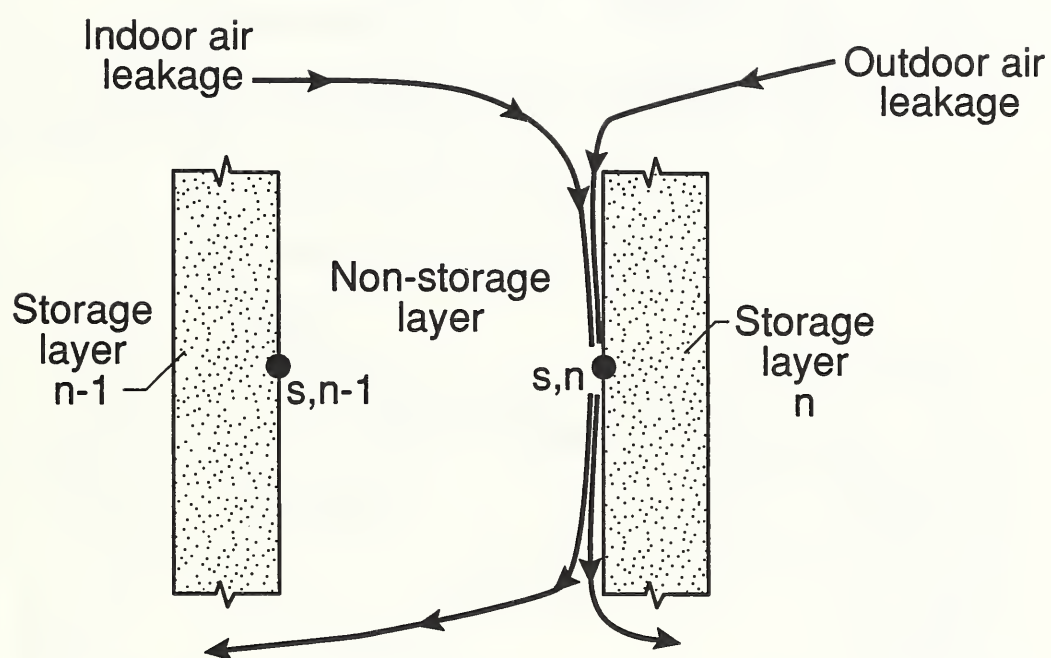
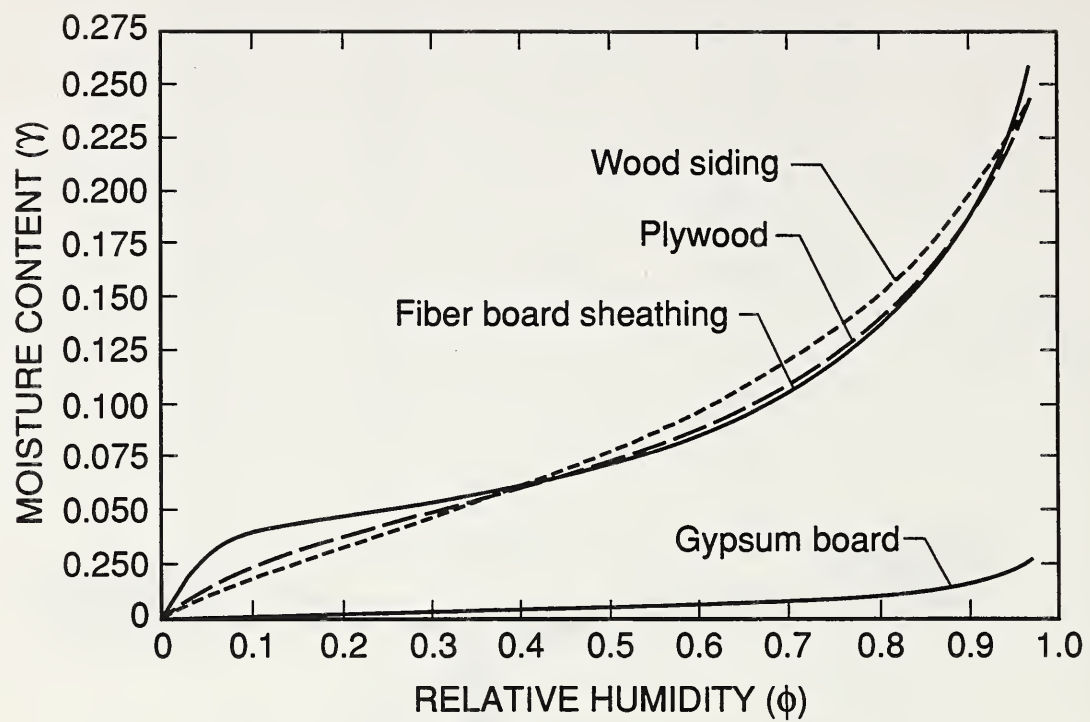
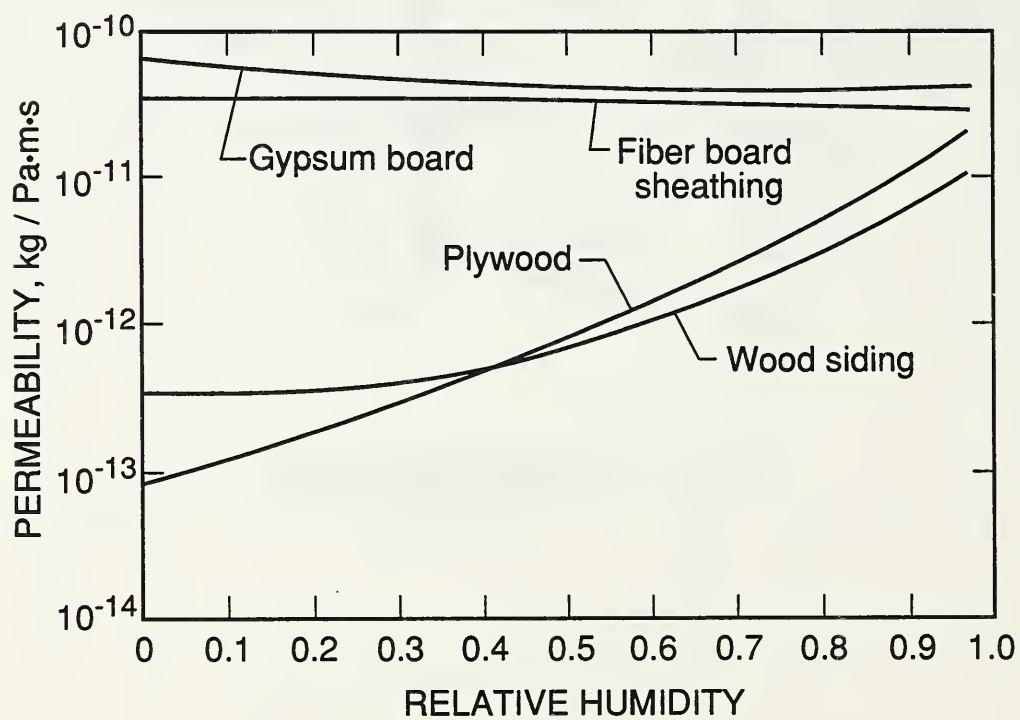


Fig 3. A non-storage layer



a. Sorption isotherms



b. Permeabilities

Fig. 4. Diffusion properties of materials used in the analysis

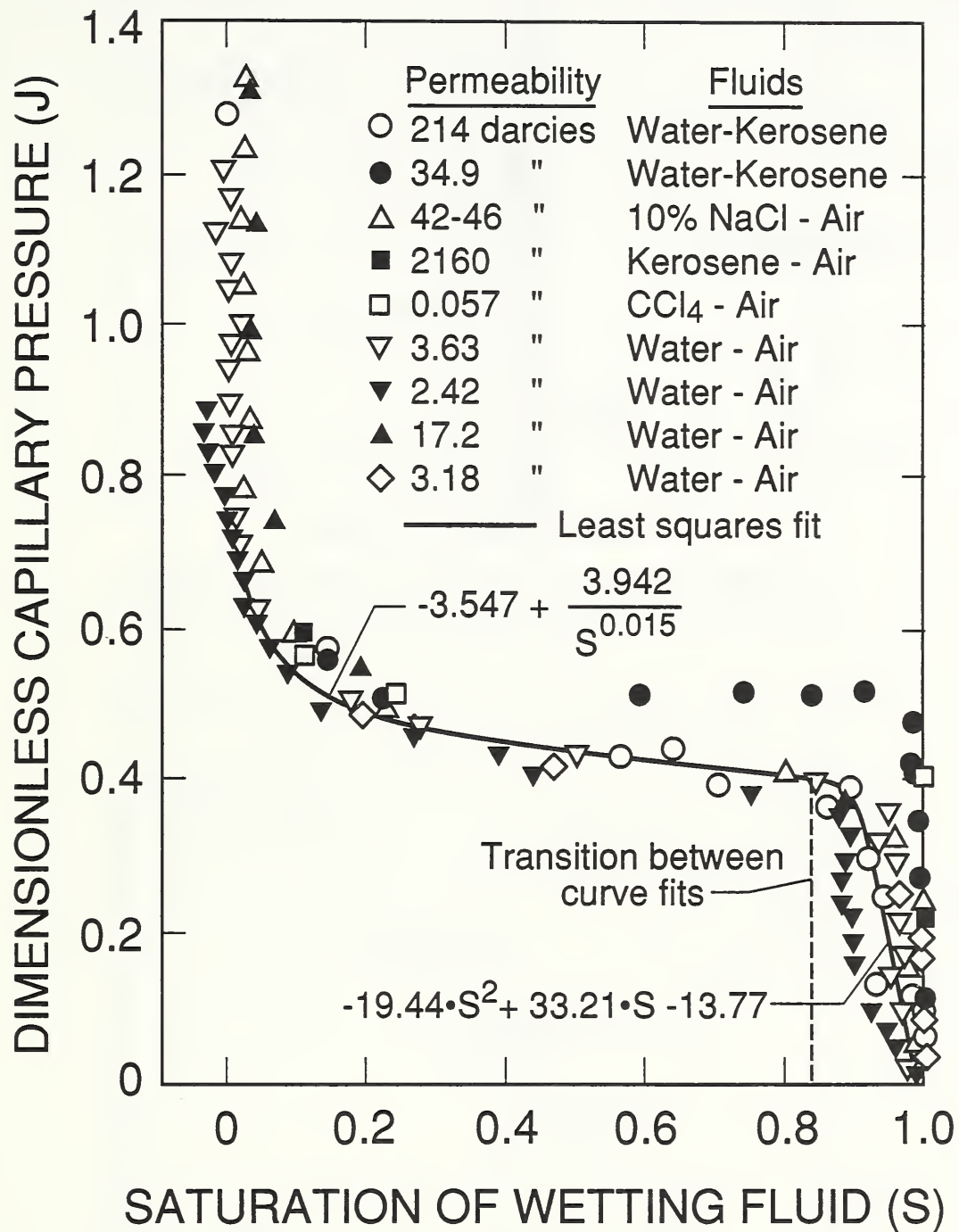
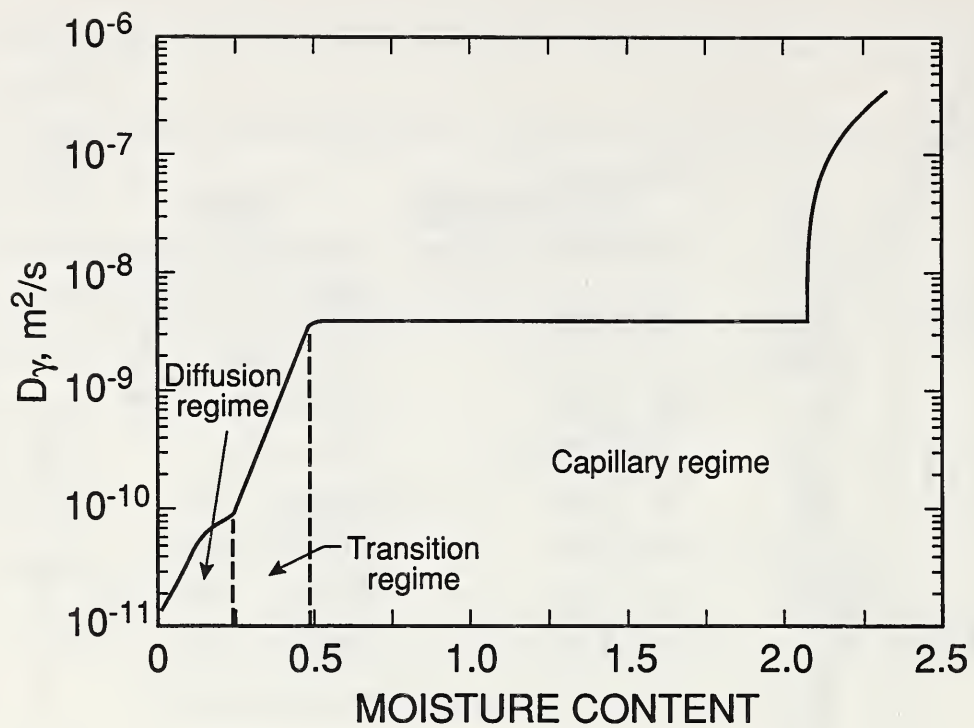
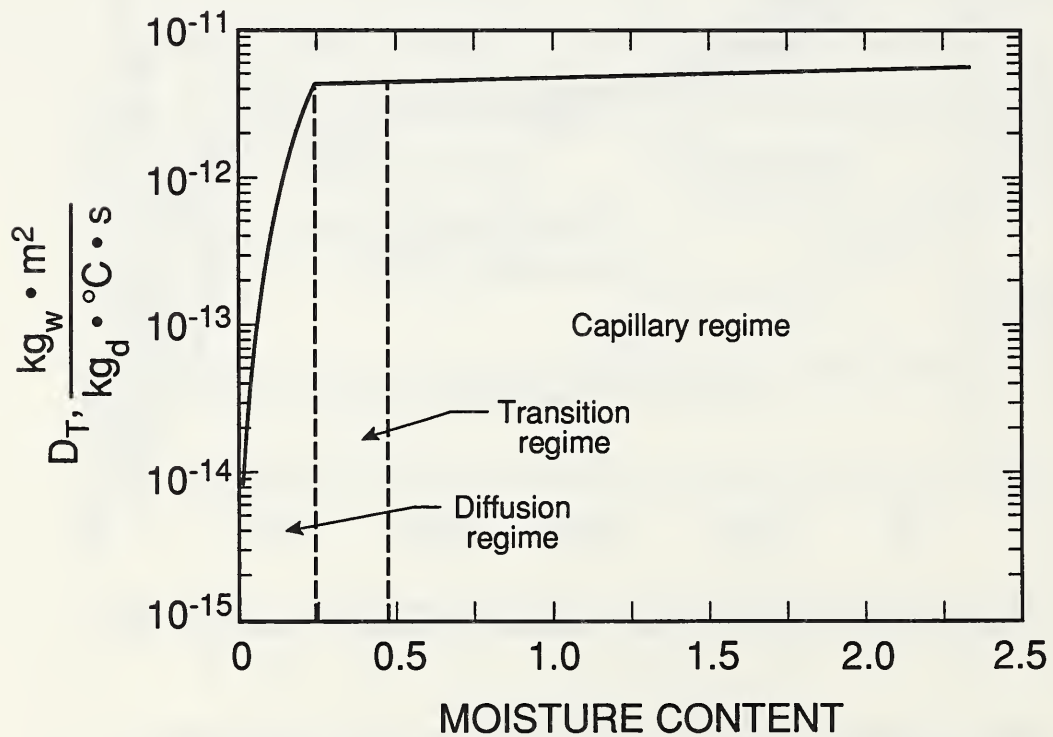


Fig. 5. Dimensionless capillary pressure versus saturation of wetting fluid for unconsolidated sands [Collins (1961)]



a. Diffusivity for the moisture content gradient



b. Diffusivity for the temperature gradient

Fig. 6. Moisture diffusivity for white pine

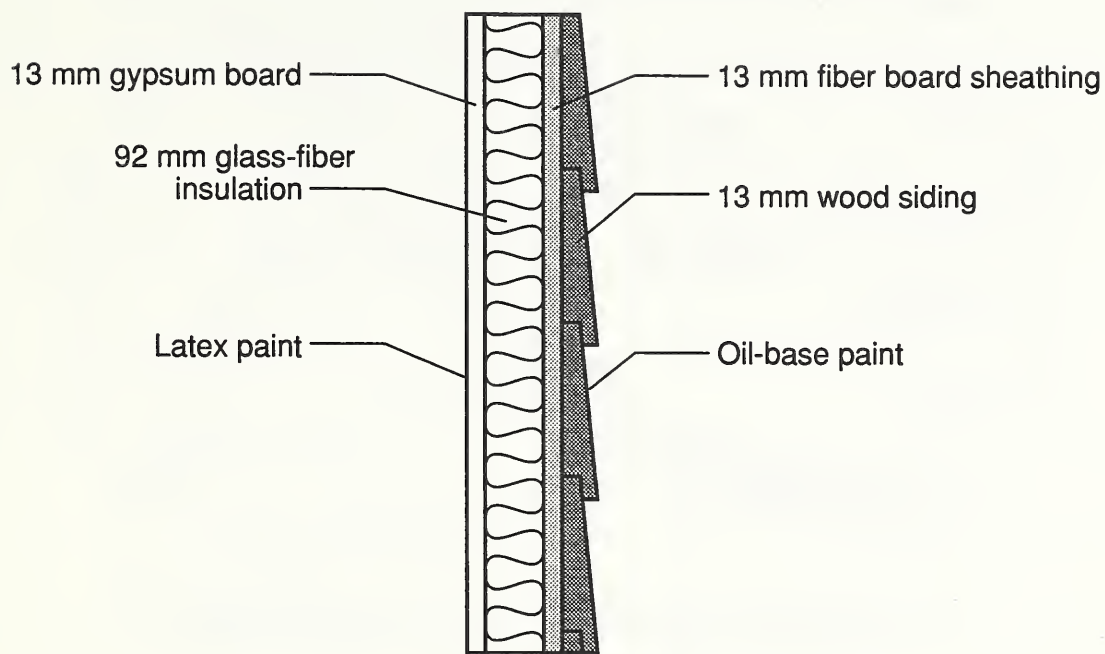


Fig. 7. Wood frame wall used in the analysis

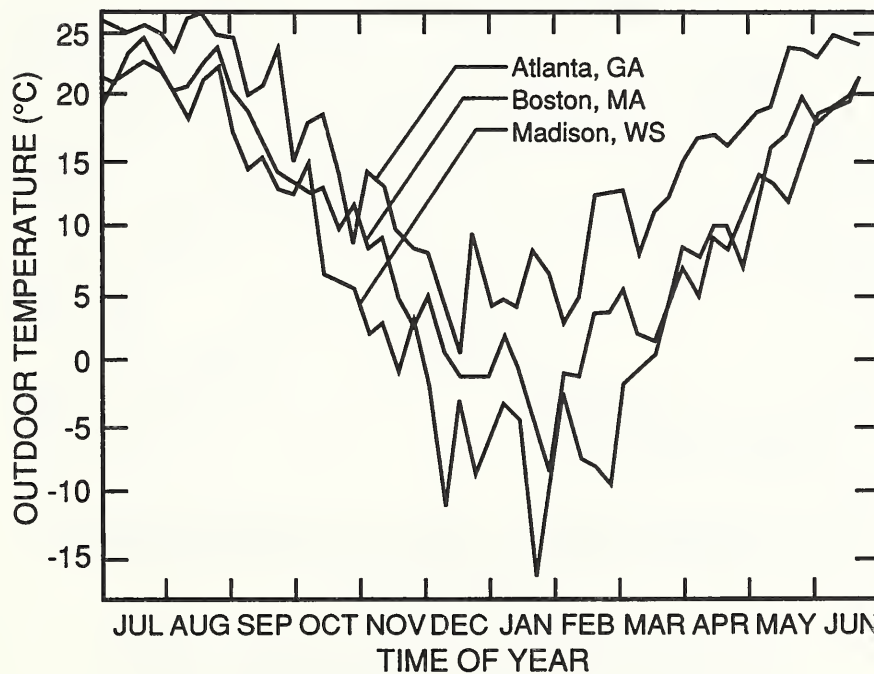
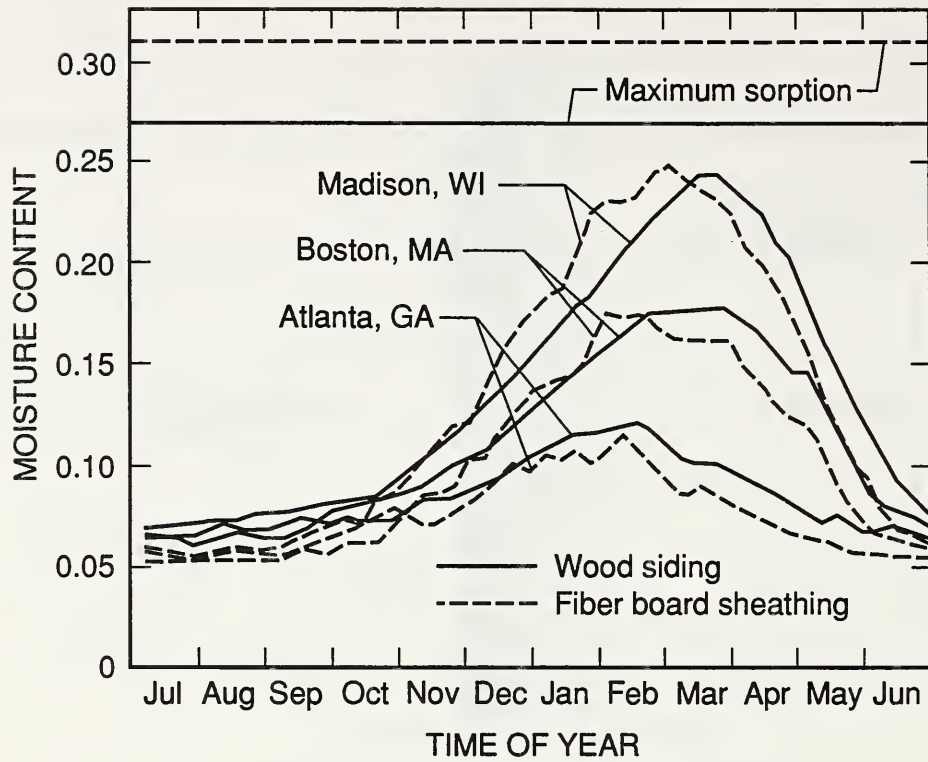
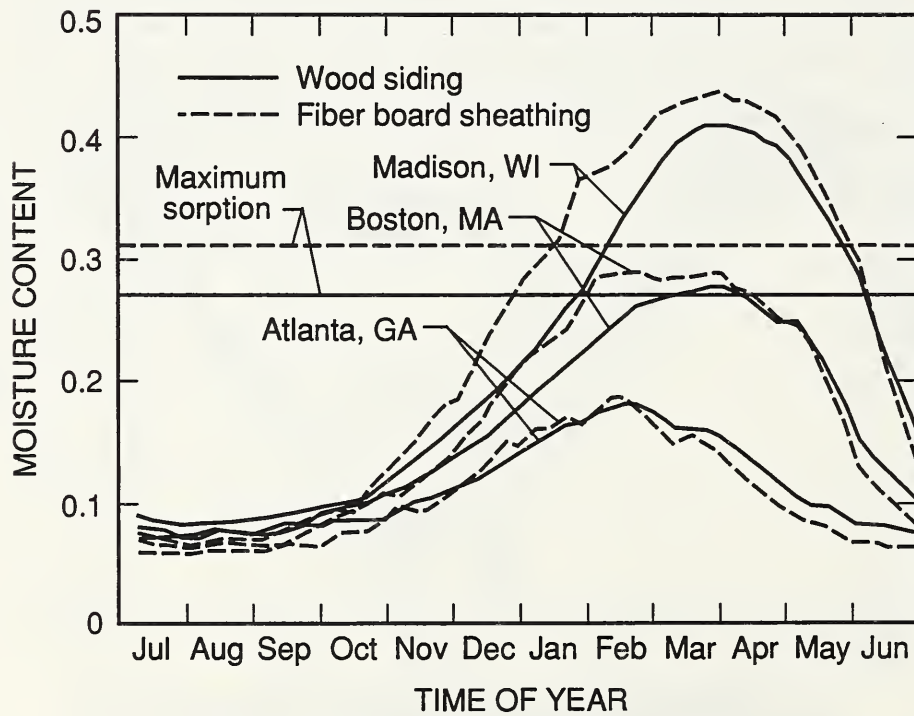


Fig. 8. Weekly average outdoor temperature for the three outdoor climates

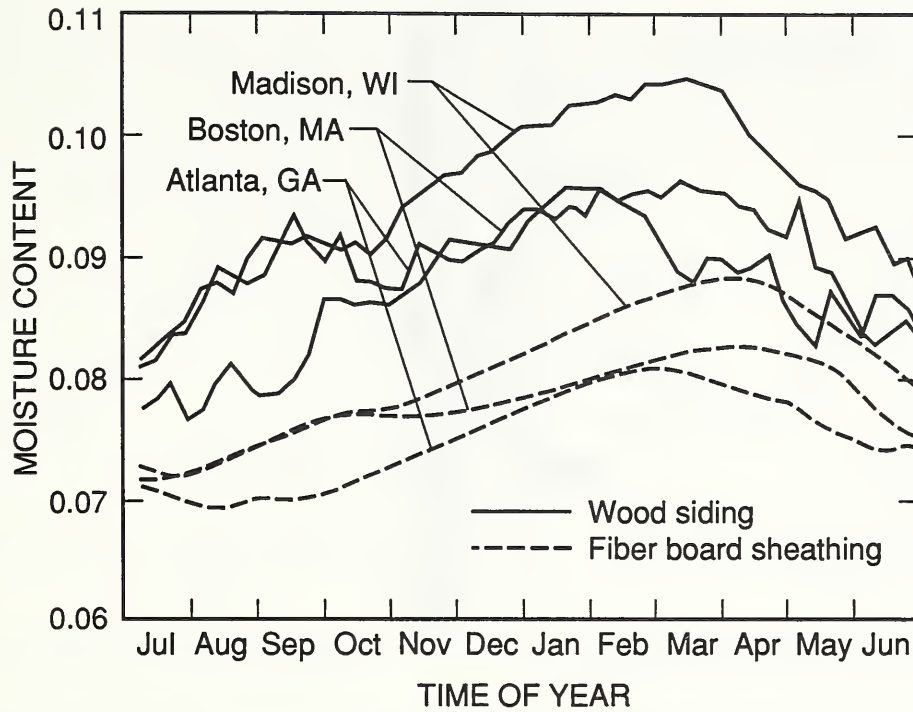


a. Indoor relative humidity, $\phi = 35\%$

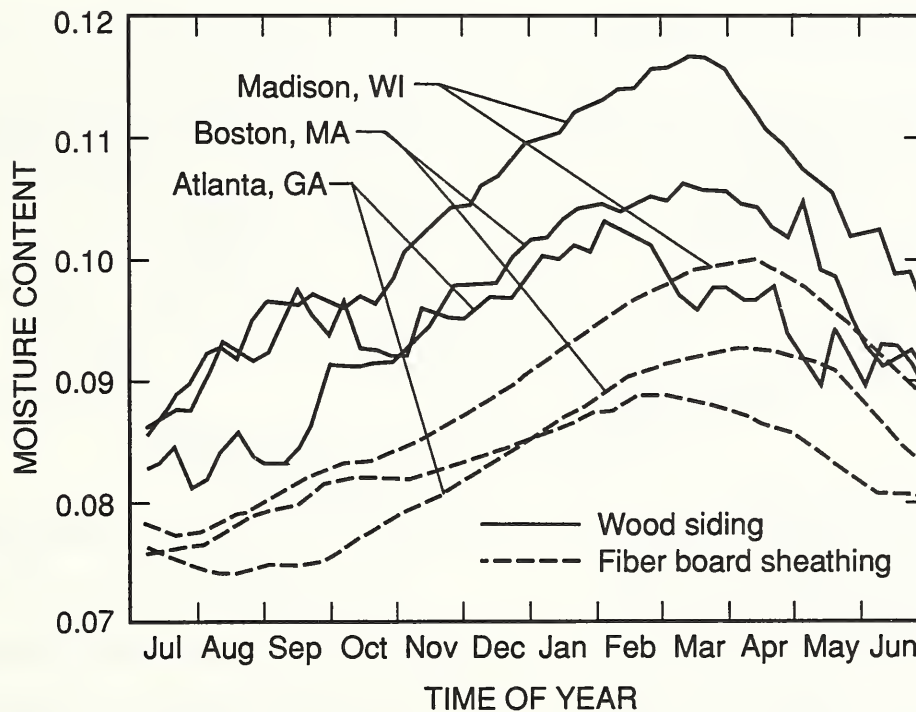


b. Indoor relative humidity, $\phi = 50\%$

Fig. 9. Moisture content plotted versus time of year for the wood frame wall without a vapor retarder and without indoor air leakage



a. Indoor relative humidity, $\phi = 35\%$



b. Indoor relative humidity, $\phi = 50\%$

Fig. 10. Moisture content plotted versus time of year for the wood frame wall with a vapor retarder and without indoor air leakage

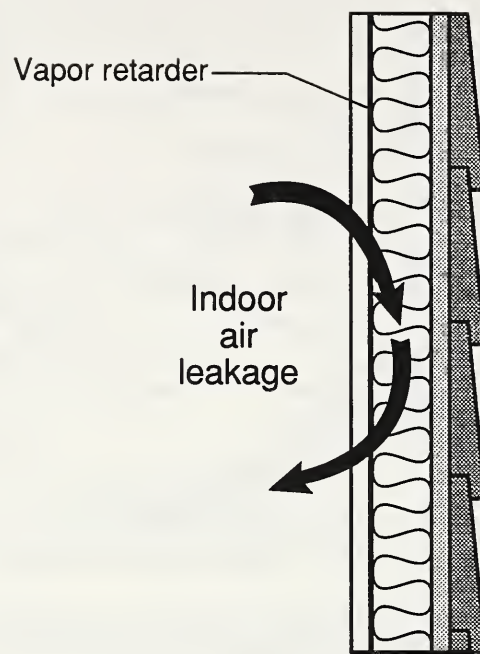
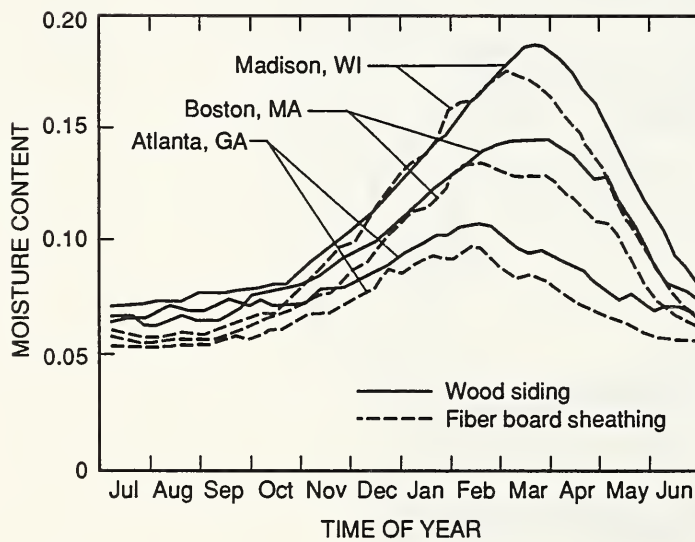
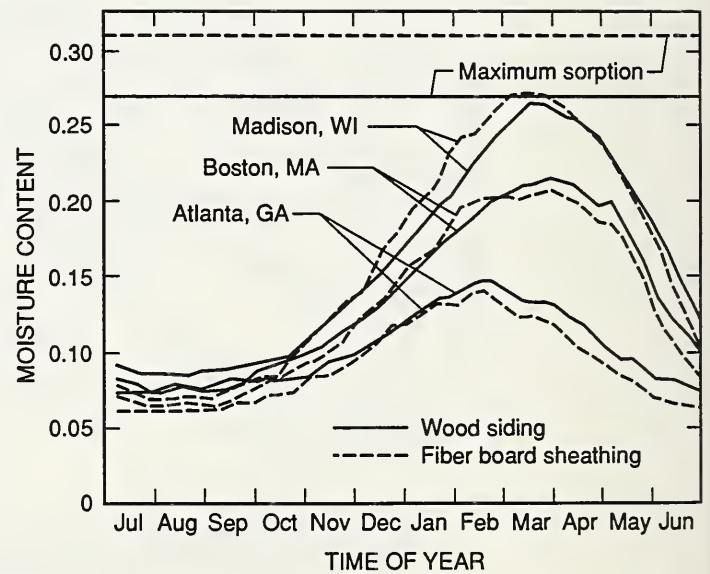


Fig. 11. Illustration of indoor air leakage into insulation cavity of wood frame wall

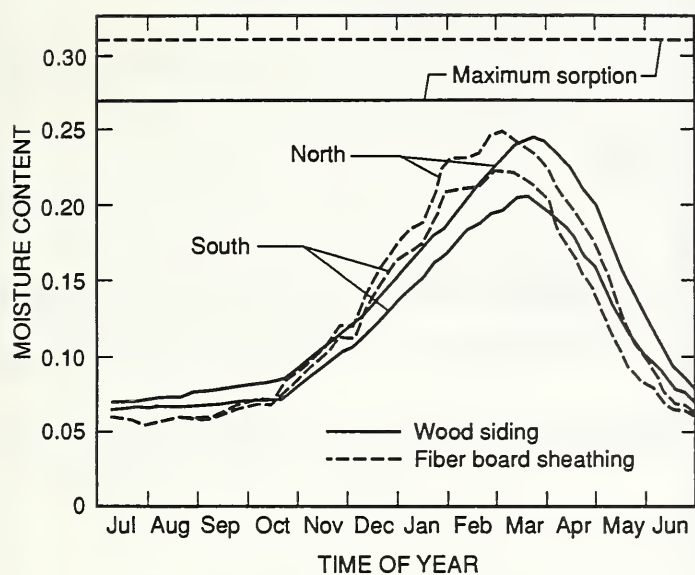


a. Indoor relative humidity, $\phi = 35\%$

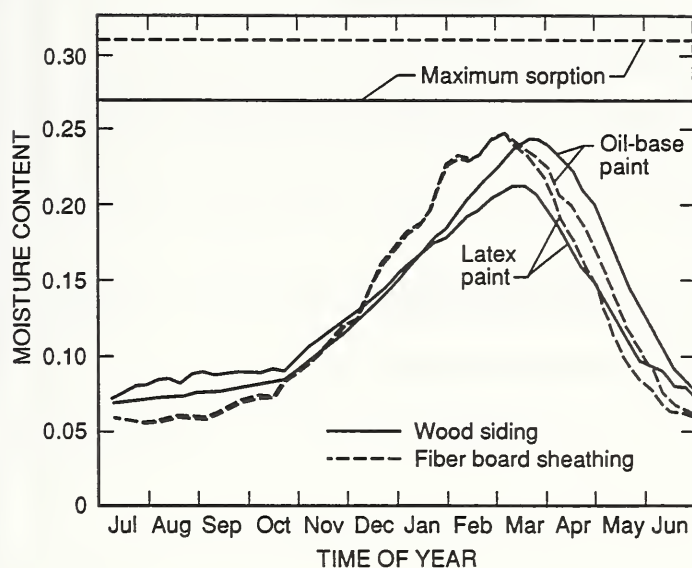


b. Indoor relative humidity, $\phi = 50\%$

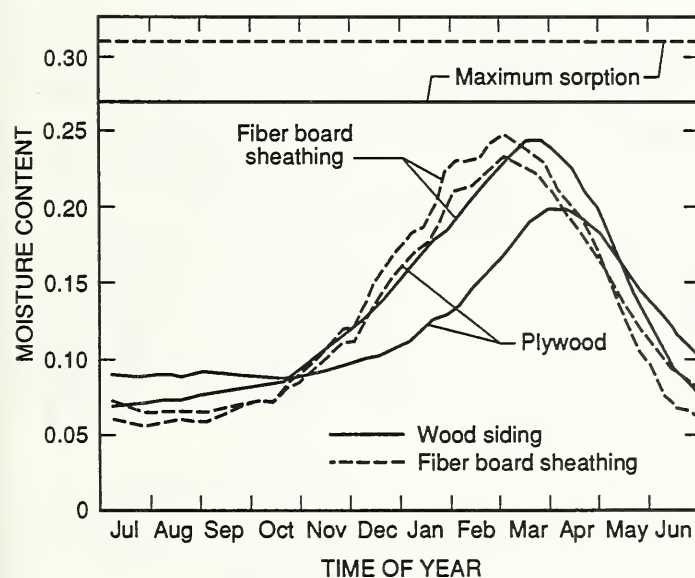
Fig. 12. Moisture content plotted versus time of year for the wood frame wall with a vapor retarder and with indoor air leakage



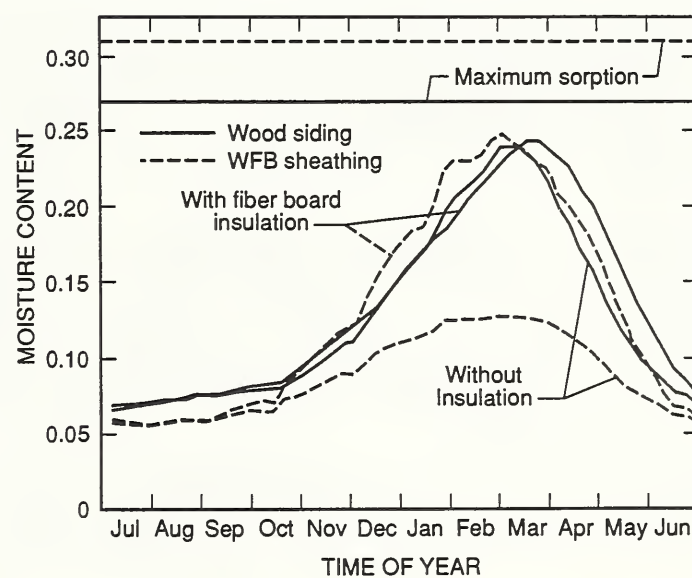
a. Effect of orientation



b. Effect of exterior paint permeance



c. Effect of sheathing permeance



d. Effect of cavity insulation

Fig. 13. Moisture content plotted versus time of year for the wood frame wall without a vapor retarder and without indoor air leakage (Madison, WI.)

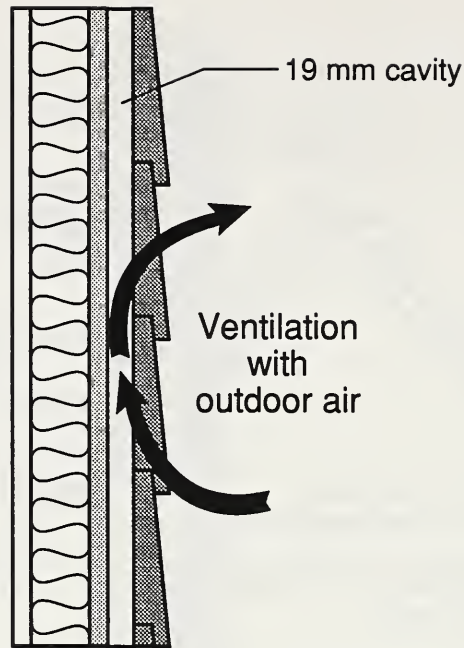
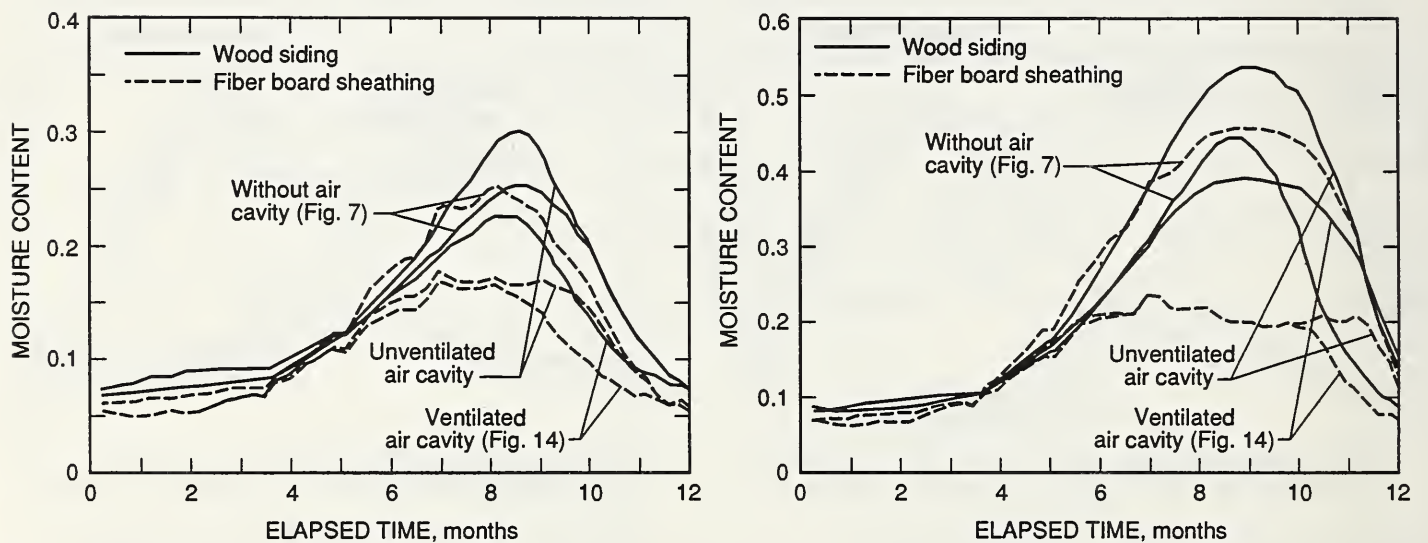


Fig. 14. Illustration of wood frame cavity wall with an exterior cavity ventilated with outdoor air



a. Indoor relative humidity, $\phi = 35\%$

b. Indoor relative humidity, $\phi = 50\%$

Fig. 15. Comparison of moisture content variation of wood frame wall without outdoor ventilation (Fig. 7) versus that of the same wood frame wall with outdoor ventilation (Fig. 14) in Madison WI.

NIST-114A (REV. 3-90)		U.S. DEPARTMENT OF COMMERCE NATIONAL INSTITUTE OF STANDARDS AND TECHNOLOGY		1. PUBLICATION OR REPORT NUMBER NISTIR 4674	
BIBLIOGRAPHIC DATA SHEET				2. PERFORMING ORGANIZATION REPORT NUMBER	
				3. PUBLICATION DATE OCTOBER 1991	
4. TITLE AND SUBTITLE An Analysis of Moisture Accumulation in A Wood-Frame Cavity Wall Subjected to Winter Climate					
5. AUTHOR(S) D. M. Burch and W. C. Thomas					
6. PERFORMING ORGANIZATION (IF JOINT OR OTHER THAN NIST, SEE INSTRUCTIONS) U.S. DEPARTMENT OF COMMERCE NATIONAL INSTITUTE OF STANDARDS AND TECHNOLOGY GAITHERSBURG, MD 20899				7. CONTRACT/GRANT NUMBER	
				8. TYPE OF REPORT AND PERIOD COVERED	
9. SPONSORING ORGANIZATION NAME AND COMPLETE ADDRESS (STREET, CITY, STATE, ZIP) U. S. Department of Energy Washington, D.C. 20585					
10. SUPPLEMENTARY NOTES					
11. ABSTRACT (A 200-WORD OR LESS FACTUAL SUMMARY OF MOST SIGNIFICANT INFORMATION. IF DOCUMENT INCLUDES A SIGNIFICANT BIBLIOGRAPHY OR LITERATURE SURVEY, MENTION IT HERE.) <p>A transient, one-dimensional, finite-difference model is presented that predicts the coupled transfer of heat and moisture in a multilayer wall under nonisothermal conditions. The model can predict moisture transfer in the diffusion through the capillary flow regimes. It has a provision to account for convective moisture transfer by including embedded cavities which may be coupled to indoor and outdoor air.</p> <p>The model is subsequently used to predict the time-varying average moisture content in the sheathing and siding of a wood frame wall as a function of time of year. Results are shown for a mild winter climate (Atlanta, GA), an intermediate winter climate (Boston, MA), and a cold winter climate (Madison, WI). The indoor temperature is maintained at 21°C, and separate computer runs are carried out for indoor relative humidities of 35% and 50%.</p> <p>The effect of several construction parameters on the winter moisture accumulation are investigated. The parameters include the interior vapor retarder permeance, sheathing permeance, exterior paint permeance, indoor air leakage, and the amount of insulation.</p>					
12. KEY WORDS (6 TO 12 ENTRIES; ALPHABETICAL ORDER; CAPITALIZE ONLY PROPER NAMES; AND SEPARATE KEY WORDS BY SEMICOLONS) capillary transfer, moisture control guidelines, moisture management in walls, moisture performance of walls, moisture transfer, water vapor diffusion					
13. AVAILABILITY <input checked="" type="checkbox"/> UNLIMITED FOR OFFICIAL DISTRIBUTION. DO NOT RELEASE TO NATIONAL TECHNICAL INFORMATION SERVICE (NTIS). <input type="checkbox"/> ORDER FROM SUPERINTENDENT OF DOCUMENTS, U.S. GOVERNMENT PRINTING OFFICE, WASHINGTON, DC 20402. <input checked="" type="checkbox"/> ORDER FROM NATIONAL TECHNICAL INFORMATION SERVICE (NTIS), SPRINGFIELD, VA 22161.				14. NUMBER OF PRINTED PAGES 36 15. PRICE A03.	

